

Multi-Switch for Antenna Selection in Massive MIMO

Xiang Gao*, Ove Edfors*, Fredrik Tufvesson*, Erik G. Larsson†

*Department of Electrical Information and Technology, Lund University, Sweden

†Department of Electrical Engineering (ISY), Linköping University, Sweden

Abstract—Massive MIMO has been shown to greatly improve spectral and transmit-energy efficiency. When implementing a massive MIMO system, one challenge is high hardware complexity. A solution is to reduce the number of radio frequency (RF) transceiver chains by performing antenna selection. However, a full RF switch that connects the antennas and RF chains can be highly complex and incurs significant loss in output signal quality, especially when the number of antennas and RF chains are large. We therefore propose a simpler solution—binary switching architecture, which is suboptimal but provides better signal quality, as compared to the full switching network. To evaluate the proposed technique, we compare the sum-rate capacity when using several different configurations of binary switching with the performance of the full switching. Full MIMO performance obtained without antenna selection is also presented as a reference. The investigations in this paper are all based on measured channel data at 2.6 GHz, using a uniform linear array and a cylindrical array, both having 128 antenna elements. It is found that the proposed binary switching gives very competitive performance that are close to the full switching, for the measured channels. The results indicate a potential to simplify massive MIMO hardware by reducing the number of RF chains, and performing antenna selection with simple binary switching architecture.

I. INTRODUCTION

Massive MIMO is an emerging technique for wireless access, where hundreds of phase-coherently operating base station antennas serve many users on the same time-frequency resource [1]–[3]. Large spatial multiplexing gains can be harvested, and transmit energy-efficiency can be improved [4]. Several experiments have confirmed that the advantages of massive MIMO, as predicted by theory, can also be achieved in real propagation channels with practical setups [5]–[9]. Massive MIMO is currently considered a leading 5G technology candidate [10], [11].

When bringing massive MIMO from theory to practice, one critical challenge is the system complexity, as the number of base station antennas and associated radio frequency (RF) chains grows to hundreds. Along with system complexity, hardware energy consumption may significantly increase, making the overall energy-efficiency of massive MIMO a question. A classical solution is antenna selection. With a large number of available antennas but fewer RF chains, antenna selection exploits the “massive” spatial degrees of freedom. Although this is not a very effective strategy for theoretical independent Rayleigh fading channels, it has been shown in [12], [13] that for real massive MIMO channels a substantial number of RF chains can be reduced without significant

performance loss. With antenna selection, an RF switching network is needed between the antennas and the RF chains. Another solution for high system complexity is hybrid precoding/beamforming [14], [15], which also deploys a limited number of RF chains but uses an RF phase-shifting network (analog precoder) instead of an RF switching network. The precoding process is therefore divided into digital baseband precoding and analog RF precoding. In comparison, antenna selection feeds the transmit energy to the “best” antennas according to a certain selection criterion, while hybrid precoding coherently processes all available antennas. Both methods need highly complex analog networks due to the large number of antennas and RF chains. In this paper, however, we do not aim for comparing the two methods. We focus on antenna selection and extend the results presented in [12], by investigating the performance of different configurations of the RF switching network.

Ideally, with antenna selection we would want M base station antennas to be served by N RF chains, connected via a full $M \times N$ switching network, as illustrated in Fig. 1. The number of possible antenna combinations is $\binom{M}{N}$. For massive MIMO where both M and N are large, however, a full RF switch potentially incurs high hardware complexity and significant loss in output signal quality, due to, e.g., insertion loss and cross-talk distortion. Especially the cross-talk distortion between the ports can be quite high, when the number of possible routes from the antennas to the RF chains becomes large. The loss in signal quality and distortion depend on the specific design of the switching network. To deal with the potential problem of high hardware complexity and signal loss, we propose a simpler solution by using binary switching per RF chain, see Fig. 2. In the simplest instance as illustrated in the figure, $M = 2N$ and each RF chain is connected to a binary switch. In total there are N binary switches, and the number of possible antenna combinations reduces to 2^N . When M and N large, $2^N \ll \binom{M}{N}$, so the hardware complexity and corresponding signal attenuation are much smaller, as compared to the full switch. A binary switch has only a fractional dB of loss. For example, the PE4259 and PE42421 UltraCMOS® RF switches have about 0.5 dB insertion loss at the 2 GHz band [16]. The signal distortion due to cross-talk and isolation coupling also reduces with the number of possible routes from the antennas to the RF chains. The drawback is the suboptimal performance due to fewer degrees of freedom in possible antenna combinations,

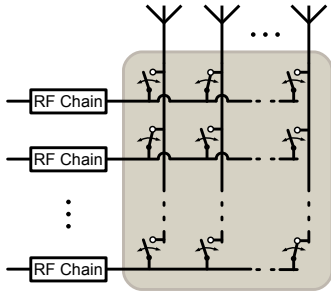


Fig. 1. A symbolic illustration of a full switching network.

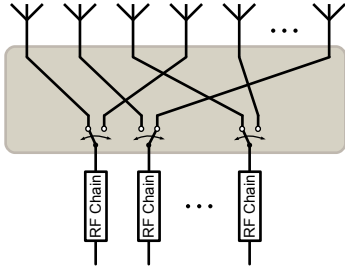


Fig. 2. A binary switching network.

as compared to full switching. However, the better signal quality of the binary switching network may compensate its performance loss, if the performance loss is not too large. In this paper, we therefore compare the performance of antenna selection with binary switching with that of full switching, based on measured massive MIMO channel data (reported and used in [5], [6], [12]), with two array types, and under different propagation conditions. As a reference, we also present full MIMO performance obtained with equal number of antennas and transceivers.

The rest of the paper is organized as follows. Sec. II gives a brief description of the massive MIMO channel data used in the study. In Sec. III we describe the system model and present the antenna selection methods with both full and binary switching. Then in Sec. IV we present performance results with the two types of switching network, and make comparisons. Summary and conclusion are given in Sec. V.

II. MEASURED CHANNELS

The channel measurements have been reported in [5], [6], [12]. Here we briefly describe the measured channels, based on which we perform antenna selection with full and binary switching.

The measured channels were obtained from two measurement campaigns, over bandwidth of 50 MHz and on the 2.6 GHz band, using two different large arrays at the base station. Both arrays contain 128 antenna elements and have an adjacent element spacing of half a wavelength at 2.6 GHz. Fig. 3a shows the cylindrical array, having 64 dual-polarized directional patch antennas, which gives a total of 128 antenna ports. This array is physically compact with both diameter and height around 30 cm. Fig. 3b shows the 7.4 m virtual linear array with a vertically-polarized omni-directional an-



Fig. 3. Two large antenna arrays at the base station side: a) a cylindrical array with 64 dual-polarized patch antennas, giving 128 ports in total, and b) a virtual linear array with 128 vertically-polarized omni-directional antennas.

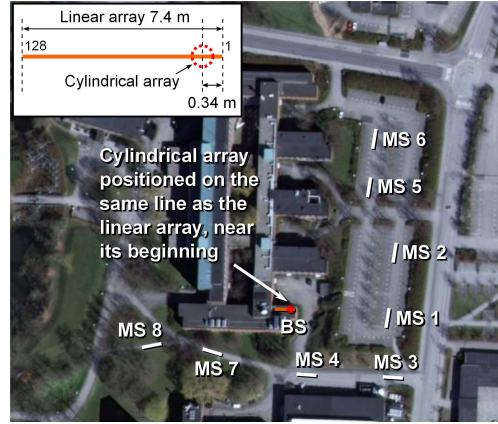


Fig. 4. Overview of the measurement area at the campus of the Faculty of Engineering (LTH), Lund University, Sweden. The two base station antenna arrays were placed on the same roof of the E-building during two measurement campaigns. Eight sites around the E-building were measured.

tenna moving along a rail, in 128 equidistant positions. In both campaigns, an omni-directional antenna with vertical polarization was used at the user side.

Both measurements were carried out outdoors at the campus of Lund University, Sweden. Fig. 4 shows an overview of the semi-urban measurement area. The two antenna arrays were placed on the same roof of the E-building during their respective measurement campaigns. At the user side, the omni-directional antenna was moved around the E-building at 8 measurement sites (MS) acting as single-antenna users. Among these sites, three (MS 1-3) have LOS conditions, and four (MS 5-8) have NLOS conditions, while one (MS 4) has LOS for the cylindrical array, but the LOS component is blocked by the roof edge for the linear array. Despite this, MS 4 still has LOS characteristic for the linear array.

III. SYSTEM DESCRIPTION AND ANTENNA SWITCHING

In our antenna selection with both full and binary switching networks, we select the set of antennas that maximizes the average downlink capacity. Here we describe the system model used in our study, and then present the selection algorithms based on convex optimization.

A. System model

We consider a single-cell multi-user MIMO-OFDM system with L subcarriers in the downlink. As shown in Fig. 5, the

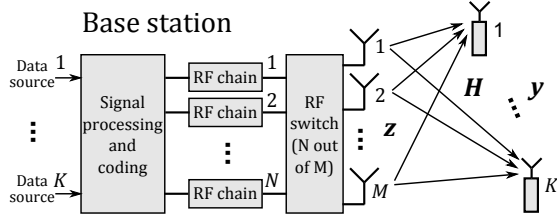


Fig. 5. System model of a multi-user MIMO system with transmit antenna selection.

base station has N RF chains and $M = 2N$ antennas, and serves K single-antenna users in the same time-frequency resource. We assume perfect channel state information (CSI) at the base station.

The model for the downlink channel is

$$\mathbf{y}_\ell = \sqrt{\frac{\rho K}{N}} \mathbf{H}_\ell^{(N)} \mathbf{z}_\ell + \mathbf{n}_\ell, \quad (1)$$

where $\mathbf{H}_\ell^{(N)}$ is a $K \times N$ channel matrix at subcarrier ℓ , and the superscript (N) represents N antennas are selected from the M . Normalization is performed such that the elements of \mathbf{H}_ℓ have unit energy, averaged over all L subcarriers, M antennas and K users, see [5] for more detail. Then \mathbf{z}_ℓ is the $N \times 1$ transmit vector across the N active antennas, and satisfies $\mathbb{E}\{\|\mathbf{z}_\ell\|^2\} = 1$, \mathbf{y}_ℓ is the received vector at the K users, and \mathbf{n}_ℓ is a white complex-Gaussian noise vector. The factor $\frac{\rho K}{N}$ represents the transmit power that increases with K and decreases with N . It means that the transmit power per user is fixed, and the array gain is harvested as reduced transmit power instead of increased receive signal-to-noise ratio (SNR) at the users. In interference-free case, the average received per-user SNR equals ρ .

With the defined model, the sum-capacity at subcarrier ℓ , achieved by dirty-paper coding (DPC) [17], is given by [18]:

$$C_{\text{DPC},\ell} = \max_{\mathbf{P}_\ell} \log_2 \det \left(\mathbf{I} + \frac{\rho K}{N} \left(\mathbf{H}_\ell^{(N)} \right)^H \mathbf{P}_\ell \mathbf{H}_\ell^{(N)} \right), \quad (2)$$

where the diagonal power allocation matrix \mathbf{P}_ℓ has $P_{\ell,i}$, $i = 1, 2, \dots, K$ on its diagonal. The maximization is performed subject to the total power constraint that $\sum_{i=1}^K P_{\ell,i} = 1$, and can be solved, for example, by using the sum-power iterative waterfilling algorithm in [19]. When performing antenna selection, we select the set that maximizes the average DPC capacity over the L subcarriers, as presented in [12], [13]:

$$\Delta_{\text{opt}} = \arg \max_{\Delta} \frac{1}{L} \sum_{\ell=1}^L \left\{ \log_2 \det \left(\mathbf{I} + \frac{\rho K}{N} \mathbf{P}_\ell \mathbf{H}_\ell \Delta \mathbf{H}_\ell^H \right) \right\}, \quad (3)$$

where Δ is an $M \times M$ diagonal matrix used for selecting N columns from the full MIMO channel matrix \mathbf{H}_ℓ , and has binary elements on its diagonal,

$$\Delta_i = \begin{cases} 1, & \text{selected} \\ 0, & \text{otherwise,} \end{cases} \quad (4)$$

indicating the i th antenna is selected or not. With the resulting antenna selection, if we apply zero-forcing (ZF) precoding in the system, we have the corresponding sum-rate

$$C_{\text{ZF},\ell} = \max_{\mathbf{Q}_\ell} \sum_{i=1}^K \log_2 \left(1 + \frac{\rho K}{N} Q_{\ell,i} \right), \quad (5)$$

subject to

$$\sum_{i=1}^K Q_{\ell,i} \left[\left(\mathbf{H}_\ell \Delta_{\text{opt}} \mathbf{H}_\ell^H \right)^{-1} \right]_{i,i} = 1, \quad (6)$$

where \mathbf{Q}_ℓ is a diagonal matrix with $Q_{\ell,i}$, $i = 1, 2, \dots, K$ on its diagonal, and $[\cdot]_{i,i}$ indicates the i -th diagonal element of a matrix. Although Δ_{opt} may not be optimal for ZF, it indicates the antenna selection performance when using more practical precoding scheme than DPC.

In the optimization process for (3), we first assume equal power allocation among users, i.e., $P_{\ell,i} = \frac{1}{K}$. After finding the optimal antenna set, we then apply the power allocation among users for each subcarrier. Next, we present how we find the optimal antenna set for both full and binary switching networks.

B. Full switching

With the full switching network as illustrated in Fig. 1, the optimization problem can be written as

$$\begin{aligned} & \text{maximize} && \frac{1}{L} \sum_{\ell=1}^L \left\{ \log_2 \det \left(\mathbf{I} + \frac{\rho}{N} \mathbf{H}_\ell \Delta \mathbf{H}_\ell^H \right) \right\}, \\ & \text{subject to} && \Delta_i \in \{0, 1\} \\ & && \sum_{i=1}^M \Delta_i = N. \end{aligned} \quad (7)$$

To solve the problem, we relax the constraint that each Δ_i must be a binary integer to a weaker constraint that $0 \leq \Delta_i \leq 1$. Then the problem becomes a convex optimization problem solvable in polynomial time [20]. The N largest Δ_i are selected, and their indices represent the selected antennas. As discussed in [12], [13], the relaxation gives near-optimal results, except for when $N \ll M$. Here we have $M = 2N$ and therefore we believe that the relaxation method is technically sound.

C. Binary switching

With binary switching, two antennas are connected with one RF chains via a binary switch, thus the antenna selection has lower degrees of freedom. There are different configurations of binary switching, depending on which two antennas are paired, see Fig. 6. Let us assume that the i th antenna and the i' th antenna ($i \neq i'$) are paired. The optimization problem for antenna selection with binary switching is

$$\begin{aligned} & \text{maximize} && \frac{1}{L} \sum_{\ell=1}^L \left\{ \log_2 \det \left(\mathbf{I} + \frac{\rho}{N} \mathbf{H}_\ell \Delta \mathbf{H}_\ell^H \right) \right\}, \\ & \text{subject to} && \Delta_i, \Delta_{i'} \in \{0, 1\} \\ & && \Delta_i + \Delta_{i'} = 1. \end{aligned} \quad (8)$$

Similar to full switching, we relax the constraint that Δ_i and $\Delta_{i'}$ being binary integers to real numbers in the interval $[0, 1]$. The problem now becomes convex. The larger one in Δ_i and $\Delta_{i'}$ is selected, and its index indicates the selected antenna.

We study three configurations of binary switching, as shown in Fig. 6. The first two are highly structured, with switching between adjacent antenna elements in Fig. 6(a) and switching between corresponding elements in sub-arrays in Fig. 6(b). The third, see Fig. 6(c), uses pseudo-random assignments of the antennas to the switches. Next, we evaluate their corresponding performance in the measured channels, for both the linear and cylindrical array.

IV. PERFORMANCE EVALUATION AND RESULTS DISCUSSION

With the measured channel data, we apply antenna selection with full and binary switching, for both arrays, in different propagation scenarios. Here we choose four scenarios to study, combining the number of users, the separation of users, and the LOS/NLOS condition. The four scenarios are:

- Four users ($K=4$) are closely located (1.5-2 m spacing) at MS 2 and all have LOS conditions to the base station.
- Four users ($K=4$) are far apart (larger than 10 m spacing) at MS 5-8 and all have NLOS conditions.
- Eight users ($K=8$) are far apart at MS 1-8 (larger than 10 m spacing), half of them have LOS conditions and half have NLOS conditions.
- Sixteen users ($K=16$) are located at MS 1-8, two users are at the same site with 5 m spacing, users at different sites have larger than 10 m spacing. Half of the users have LOS conditions and half have NLOS conditions.

The parameter setting for evaluating antenna selection performance with different switching configurations is as follows. We have $M=128$ base station antennas and $N=64$ RF chains, so we select the 64 antennas that maximize the average DPC capacity over all $L=161$ subcarriers. The number of users, K , is 4, 8 and 16, as mentioned above. We set the interference-free per-user SNR, ρ , to be in the range of -10 dB to 20 dB. We also evaluate the full MIMO performance without antenna selection and switching, when $M=N=128$ and 64, and make comparisons with the antenna selection performance. With 64 antennas and 64 RF chains, we select all realizations of 64 adjacent elements on the arrays, and evaluate the average sum-rate performance. With 128 antennas and 128 RF chains, for a fair comparison, we have the same amount of transmit power as the cases when $N=64$.

For the linear array, with the switching configuration in Fig. 6(a) we pair the adjacent elements, with the configuration in Fig. 6(b) we pair the two elements that are separated by 64 antennas. For the cylindrical array, with the configuration in Fig. 6(a) we pair the adjacent elements that are the vertically and horizontally-polarized ports of the same patch (see Fig. 3). With the configuration in Fig. 6(b), we pair the two elements with the same polarization and on the same circle but facing the opposite directions. For both arrays with the configuration

in Fig. 6(c), we randomly generate 1000 realizations of pairing, and evaluate their average performance. We present and discuss the performance evaluation results in the following.

Due to limited space in the paper, we only show the DPC capacities in the LOS scenario where four users are closely located, see Fig. 7 and Fig. 8, and in the scenario where sixteen users are distributed around the base station, see Fig. 9 and Fig. 10, for the linear and cylindrical arrays, respectively. For all the scenarios with DPC and ZF, we summarize the results in Table I and II for the linear array, Table III and IV for the cylindrical array.

We first pay attention to the LOS scenario where four users are closely located, as shown in Fig. 7 and Fig. 8, for the linear and cylindrical arrays, respectively. In the two figures, the performance loss when using the proposed binary switching is only marginal, compared with the full switching. The differences in performance between different binary switching configurations are very small. The adjacent-element switching in Fig. 6(a) gives slightly worse performance than the other two configurations. This is because the spatial diversity between adjacent antennas is usually small, as compared to the spatial diversity between separated elements.

We also compare the antenna selection performance with the full MIMO performance for $M=N=64$ and 128. The full MIMO performance of 64 antennas and RF chains is used as a benchmark. Based on that, if we add another 64 antennas and an RF switch network, we gain 2.5-3 dB in SNR with the linear array, and 1.5-3 dB with the cylindrical array, when $\rho=10$ dB. If we add 64 antennas and 64 RF chains, we gain 5 dB in SNR with the linear array, and 3.5 dB with the cylindrical array. Adding RF chains, however, is usually expensive and leads to high hardware complexity and energy consumption. In this scenario, adding more antennas and an RF switch and performing antenna selection may be an economic solution to boost the system performance.

We turn to the scenario with sixteen users, as shown in Fig. 9 and Fig. 10. In this scenario, the binary switching again performs very close to the full switching. The differences in performance between the three binary switching configurations are quite small. When comparing with the full MIMO performance with 64 antennas and RF chains, we find that by adding another 64 antennas and an RF switch, we gain 1-1.5 dB and 1-2 dB in SNR, with the linear and cylindrical arrays, respectively. By adding 64 antennas and 64 RF chains, we then gain 4 dB in SNR with both arrays. In this scenario, we do not gain as much as in the previous scenario by performing antenna selection. This is because that with more users more active antennas and RF chains are required to spatially separate the users and further improve the performance, as discussed in more detail in [12].

The results for the four scenarios with DPC and ZF are summarized in Table I and II for the linear array, and Table III and IV, for the cylindrical array. We illustrate the performance gain in SNR compared with the average full MIMO performance of 64 antennas and 64 RF chains, when increasing to 128 antennas and performing antenna selection using different

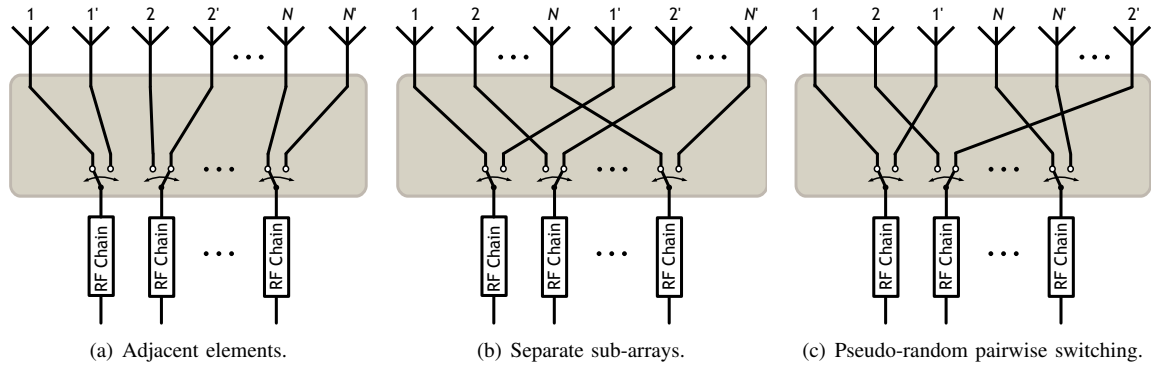


Fig. 6. Three example configurations of the proposed binary switching solution (for $M = 2N$).

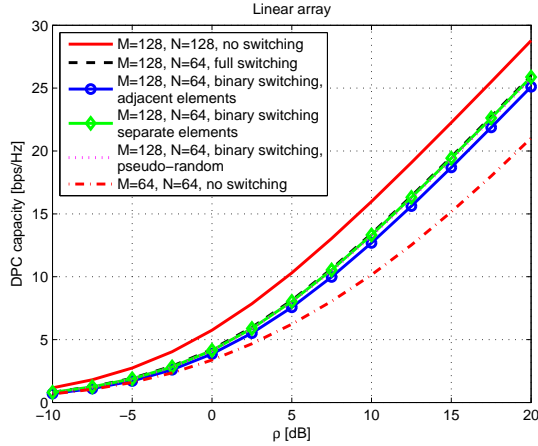


Fig. 7. Performance comparison in the LOS scenario where four users are closely located at MS 2, with the linear array at the base station.

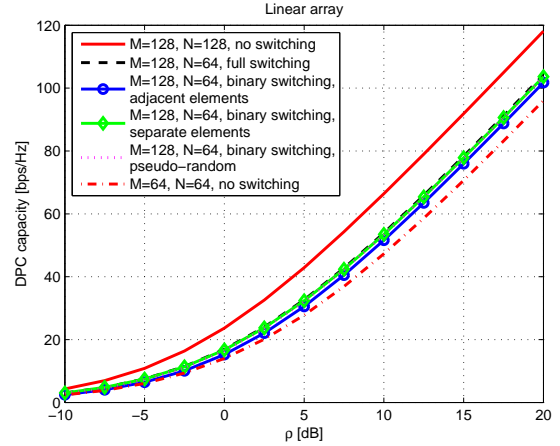


Fig. 9. Performance comparison in the scenario where sixteen users are distributed at MS 1-8, half have LOS conditions and half have NLOS conditions, with the linear array at the base station.

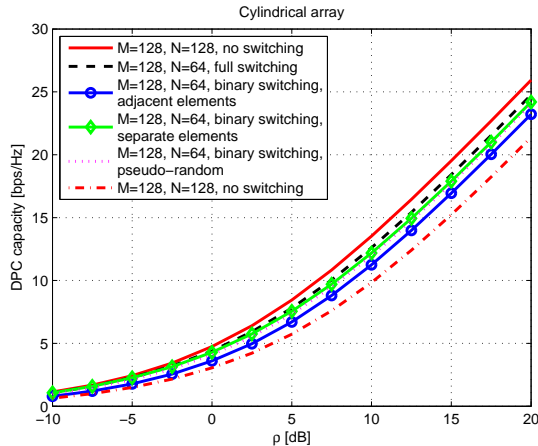


Fig. 8. Performance comparison in the LOS scenario where four users are closely located at MS 2, with the cylindrical array at the base station.

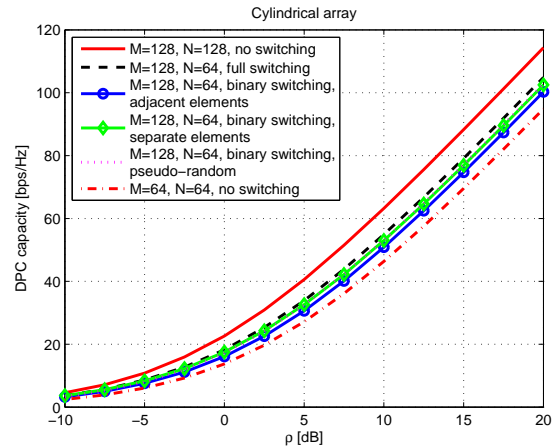


Fig. 10. Performance comparison in the scenario where sixteen users are distributed at MS 1-8, half have LOS conditions and half have NLOS conditions, with the cylindrical array at the base station.

switching networks, and when increasing to 128 antennas and 128 RF chains. We see that the binary switching performs very close to the full switching, in all cases, for both DPC and ZF, and for both arrays. This indicates a potential to use the simple binary switching instead of the complex full switching. Compared with the full MIMO with 64 antennas and RF chains, we do not gain significantly by adding antennas and performing antenna selection on the linear array, in the case of well-separated users in NLOS conditions. In this case the

channel provides more “favorable” propagation, and the full MIMO performance is fairly good. However, in the relatively difficult scenario for spatial separation of users, e.g., when users are closely located in LOS conditions, we can boost the performance by adding more antennas and performing antenna selection. With antenna selection on the cylindrical array, the performance gain is significant in all scenarios.

TABLE I
THE PERFORMANCE GAIN WITH DPC, COMPARED WITH 64 ANTENNAS
AND 64 RF CHAINS, USING THE LINEAR ARRAY, AT $\rho = 10$ dB.

Scenario	128 ant. 128 RF	128 ant. and 64 RF with switching			
		Full	Binary a	Binary b	Binary c
4 users, LOS co-located	5 dB	3 dB	2.5 dB	~ 3 dB	~ 3 dB
4 users, NLOS well-separated	4 dB	1 dB	0.5 dB	~ 1 dB	~ 1 dB
8 users	3.5 dB	1 dB	0.5 dB	~ 1 dB	~ 1 dB
16 users	4 dB	1.5 dB	1 dB	~ 1.5 dB	~ 1.5 dB

The symbol \sim presents that the gain is very close to a certain dB.

TABLE II
THE PERFORMANCE GAIN WITH ZF, COMPARED WITH 64 ANTENNAS AND
64 RF CHAINS, USING THE LINEAR ARRAY, AT $\rho = 10$ dB.

Scenario	128 ant. 128 RF	128 ant. and 64 RF with switching			
		Full	Binary a	Binary b	Binary c
4 users, LOS co-located	8 dB	~ 6 dB	5 dB	6 dB	~ 6 dB
4 users, NLOS well-separated	3.5 dB	1 dB	0.5 dB	~ 1 dB	~ 1 dB
8 users	3.5 dB	1 dB	0.5 dB	~ 1 dB	~ 1 dB
16 users	5 dB	2 dB	1.5 dB	~ 2 dB	~ 2 dB

V. SUMMARY AND CONCLUSION

In this paper we have analyzed a simplified antenna selection scheme for massive MIMO. The presented technique could make antenna selection in massive MIMO feasible. As demonstrated by the experimental results, in many scenarios only a subset of the antennas actually contributes to the achieved sum-rate. This means that by exploiting the large spatial degrees of freedom, the number of actual transceivers can be reduced without significant performance loss. Furthermore, as also demonstrated by the experimental results, performing the antenna selection using the proposed binary switching circumvents the high complexity and corresponding losses in signal quality associated with a full RF switch, without appreciably sacrificing performance. All these results indicate

TABLE III
THE PERFORMANCE GAIN WITH DPC, COMPARED WITH 64 ANTENNAS
AND 64 RF CHAINS, USING THE CYLINDRICAL ARRAY, AT $\rho = 10$ dB.

Scenario	128 ant. 128 RF	128 ant. and 64 RF with switching			
		Full	Binary a	Binary b	Binary c
4 users, LOS co-located	3.5 dB	3 dB	1.5 dB	2.5 dB	~ 2.5 dB
4 users, NLOS well-separated	3.5 dB	2.5 dB	2 dB	1.5 dB	2 dB
8 users	3.5 dB	2 dB	1.5 dB	~ 2 dB	~ 2 dB
16 users	4 dB	2 dB	1 dB	1.5 dB	1.5 dB

TABLE IV
THE PERFORMANCE GAIN WITH ZF, COMPARED WITH 64 ANTENNAS AND
64 RF CHAINS, USING THE CYLINDRICAL ARRAY, AT $\rho = 10$ dB.

Scenario	128 ant. 128 RF	128 ant. and 64 RF with switching			
		Full	Binary a	Binary b	Binary c
4 users, LOS co-located	~ 4 dB	2.5 dB	~ 1.5 dB	~ 2 dB	~ 2 dB
4 users, NLOS well-separated	3.5 dB	2 dB	~ 2 dB	1.5 dB	~ 2 dB
8 users	~ 4 dB	2 dB	1 dB	1.5 dB	1.5 dB
16 users	4.5 dB	2 dB	~ 1.5 dB	~ 1.5 dB	1.5 dB

a potential to greatly simplify massive MIMO hardware.

ACKNOWLEDGEMENT

The authors would like to acknowledge the support from ELLIIT - an Excellence Center at Linköping-Lund in Information Technology, the Swedish Research Council (VR) and the Swedish Foundation for Strategic Research (SSF). The research leading to these results has received funding from the European Union Seventh Framework Programme (FP7/2007-2013) under grant agreement n^o 619086 (MAMMOET).

REFERENCES

- [1] F. Rusek, D. Persson, B. K. Lau, E. G. Larsson, T. L. Marzetta, O. Edfors, and F. Tufvesson, "Scaling up MIMO: Opportunities and challenges with very large arrays," *IEEE Signal Process. Mag.*, vol. 30, no. 1, Jan. 2013.
- [2] E. Larsson, O. Edfors, F. Tufvesson, and T. Marzetta, "Massive MIMO for next generation wireless systems," *IEEE Commun. Mag.*, vol. 52, no. 2, pp. 186–195, Feb. 2014.
- [3] T. L. Marzetta, "Noncooperative cellular wireless with unlimited numbers of base station antennas," *IEEE Trans. Wireless Commun.*, vol. 9, no. 11, pp. 3590–3600, Nov. 2010.
- [4] H. Q. Ngo, E. G. Larsson, and T. L. Marzetta, "Energy and spectral efficiency of very large multiuser MIMO systems," *IEEE Trans. Commun.*, vol. 61, no. 4, pp. 1436–1449, Apr. 2013.
- [5] X. Gao, O. Edfors, F. Rusek, and F. Tufvesson, "Massive MIMO performance evaluation based on measured propagation data," *IEEE Trans. Wireless Commun.*, vol. 14, no. 7, pp. 3899–3911, July 2015.
- [6] X. Gao, F. Tufvesson, O. Edfors, and F. Rusek, "Measured propagation characteristics for very-large MIMO at 2.6 GHz," in *Proc. 46th Asilomar*, Nov. 2012, pp. 295–299.
- [7] X. Gao, O. Edfors, F. Rusek, and F. Tufvesson, "Linear pre-coding performance in measured very-large MIMO channels," in *Proc. IEEE VTC-Fall*, Sep. 2011, pp. 1–5.
- [8] J. Hoydis, C. Hoek, T. Wild, and S. ten Brink, "Channel measurements for large antenna arrays," in *Proc. ISWCS*, Aug. 2012, pp. 811–815.
- [9] J. Flordelis, X. Gao, G. Dahman, F. Rusek, O. Edfors, and F. Tufvesson, "Spatial separation of closely-spaced users in measured massive multi-user MIMO channels," in *Proc. IEEE ICC*, June 2015.
- [10] J. Andrews, S. Buzzi, W. Choi, S. Hanly, A. Lozano, A. Soong, and J. Zhang, "What will 5G be?" *IEEE J. Sel. Areas Commun.*, vol. 32, no. 6, pp. 1065–1082, June 2014.
- [11] F. Boccardi, R. Heath, A. Lozano, T. Marzetta, and P. Popovski, "Five disruptive technology directions for 5G," *IEEE Commun. Mag.*, vol. 52, no. 2, pp. 74–80, Feb. 2014.
- [12] X. Gao, O. Edfors, F. Tufvesson, and E. G. Larsson, "Massive MIMO in real propagation environments: Do all antennas contribute equally?" *IEEE Trans. Commun.*, 2015.
- [13] X. Gao, O. Edfors, J. Liu, and F. Tufvesson, "Antenna selection in measured massive MIMO channels using convex optimization," in *Proc. IEEE GlobeCom Workshop on Emerging Technologies for LTE-Advanced and Beyond-4G*, Dec. 2013.
- [14] F. Khalid and J. Speidel, "Robust hybrid precoding for multiuser MIMO wireless communication systems," *IEEE Trans. Wireless Commun.*, vol. 13, no. 6, pp. 3353–3363, June 2014.
- [15] L. Liang, W. Xu, and X. Dong, "Low-complexity hybrid precoding in massive multiuser MIMO systems," *IEEE Wireless Commun. Lett.*, vol. 3, no. 6, pp. 653–656, Dec. 2014.
- [16] Peregrine Semiconductor. [Online]. Available: <http://www.psemi.com/>
- [17] M. Costa, "Writing on dirty paper," *IEEE Trans. Inf. Theory*, vol. 29, no. 3, pp. 439–441, 1983.
- [18] S. Vishwanath, N. Jindal, and A. Goldsmith, "Duality, achievable rates, and sum-rate capacity of Gaussian MIMO broadcast channels," *IEEE Trans. Inf. Theory*, vol. 49, no. 10, pp. 2658–2668, Oct. 2003.
- [19] N. Jindal, W. Rhee, S. Vishwanath, S. Jafar, and A. Goldsmith, "Sum power iterative water-filling for multi-antenna Gaussian broadcast channels," *IEEE Trans. Inf. Theory*, vol. 51, no. 4, pp. 1570–1580, Apr. 2005.
- [20] S. Boyd and L. Vandenberghe, *Convex Optimization*. Cambridge University Press, 2004.